



Published in final edited form as:

J Med Chem. 2013 April 11; 56(7): 2936–2947. doi:10.1021/jm301890k.

Amino acid conjugates of lithocholic acid as antagonists of the EphA2 receptor

Matteo Incerti^{‡,1}, Massimiliano Tognolini^{*‡,1}, Simonetta Russo¹, Daniele Pala¹, Carmine Giorgio¹, Iftiin Hassan-Mohamed¹, Roberta Noberini², Elena B. Pasquale², Paola Vicini¹, Silvia Piersanti¹, Silvia Rivara¹, Elisabetta Barocelli¹, Marco Mor¹, and Alessio Lodola^{*,1}

¹Dipartimento di Farmacia, Università degli Studi di Parma, Viale delle Scienze 27/A, I-43124 Parma, Italy

²Sanford-Burnham Medical Research Institute, 10901 North Torrey Pines Road, La Jolla, CA 92037, USA.

Abstract

The Eph receptor–ephrin system is an emerging target for the development of novel antiangiogenetic agents. We recently identified lithocholic acid (LCA) as a small molecule able to block EphA2-dependent signals in cancer cells, suggesting that its (5 β)-cholan-24-oic acid scaffold can be used as a template to design a new generation of improved EphA2 antagonists. Here, we report the design and synthesis of an extended set of LCA derivatives obtained by conjugation of its carboxyl group with different α -amino acids. Structure-activity relationships indicate that the presence of a lipophilic amino acid side chain is fundamental to achieve good potencies. The L-Trp derivative (**20**, PCM126) was the most potent antagonist of the series disrupting EphA2-ephrinA1 interaction and blocking EphA2 phosphorylation in prostate cancer cells at low μ M concentrations, thus being significantly more potent than LCA. Compound **20** is among the most potent small molecule antagonists of the EphA2 receptor.

INTRODUCTION

The erythropoietin-producing hepatocellular carcinoma (Eph) receptors are the largest family of receptor tyrosine kinases and together with their ligands, the ephrins, represent a distinctive communication system in which both ligands and receptors are bound to membrane and initiate bidirectional cell-cell signaling.¹ Indeed, the Eph receptor-ephrin system can both transduce “forward” signals into Eph receptor-expressing cells and “reverse” signals into the cells where the ephrins are expressed.²

Fourteen Eph receptors (divided in the EphA and EphB classes) and eight ephrins (also divided in A and B classes, corresponding to their affinities for the Eph receptor sub-families) have been so far identified in humans.³ Given their membrane localization, these proteins can modulate a large and diverse array of biological functions including organ development, tissue remodeling, neuronal signaling, insulin secretion, blood haemostasis and bone metabolism.^{4,5} Not surprisingly, dysregulation of the Eph-ephrin signaling system

*Corresponding Author Alessio Lodola Phone: +39 0521 905062 Fax: +39 0521 905006 alessio.lodola@unipr.it Massimiliano Tognolini Phone : +39 0521 906021 Fax: : +39 0521 905091 massimiliano.tognolini@unipr.it

[‡]These authors contributed equally to this work.

Supporting Information Plot of experimental pIC₅₀ vs MM-PBSA binding energy. LDH assay for compound **20**. Characterization data for compound **2-21**, including mp, ¹H-NMR and ¹³C-NMR, MS data, and the results of elemental analysis. This material is available free of charge via the Internet at <http://pubs.acs.org>.

has been implicated in pathological conditions related to all of these systems.⁵ In particular, the involvement of Eph/ephrin signaling in tumorigenesis has been extensively investigated due to recurrent up-regulation of Eph receptors in several types of human cancers.⁶⁻⁸ Despite these findings, the roles played by Eph receptors in tumor progression remain unclear, due to the diverse biological functions associated with individual Eph receptors and ephrin ligands, including oncogenic or tumor suppressor functions.⁹⁻¹¹

From a therapeutic perspective, targeting the Eph receptors appears straightforward in the context of inhibiting Eph/ephrin-signaling in the vasculature as a mean of preventing tumor angiogenesis.¹¹ Indeed, inhibition of EphA2 and EphB4 has been shown to effectively block angiogenic processes *in vivo*.^{6,12} Furthermore, it has been recently shown that the EphA2 receptor can be exploited to deliver anticancer drugs into EphA2-expressing cancer cells, by using targeting peptides.¹³

Two main strategies can be used to inhibit Eph receptor dependent signals:^{6,14} *i*) blockage of Eph receptor forward signaling by a direct action on the ATP-binding pocket in the receptor kinase domain;¹⁵⁻¹⁷ *ii*) blockage of both Eph receptor forward and ephrin reverse signals by disruption of the Eph receptor–ephrin interaction.¹⁸ While the first approach is based on the use of small molecules inhibiting the ATP binding site in the intracellular kinase domain, the second one is based on the use of recombinant proteins (soluble forms of Eph receptors and ephrins), antibodies and peptides.¹⁸

The discovery of small molecules able to disrupt protein–protein interaction remains a challenging task for medicinal chemistry, mainly because the contact surfaces involved in protein–protein interactions are large (~1,500–3,000 Å²) compared with those usually involved in protein–small-molecule interactions (~300–1,000 Å²).¹⁹ Nevertheless, the ephrin-binding site of Eph receptors presents favorable features for high affinity binding of small molecules. Indeed, different classes of low-molecular weight compounds able to interfere with the binding of ephrins to Eph receptors have been recently identified (Figure 1). These include: *i*) bile acid derivatives, such as lithocholic acid (LCA, compound **1**)^{20,21} and cholanic acid,²² two competitive Eph receptor antagonists having a moderate preference for the EphA receptor subfamily; *ii*) salicylic-acid derivatives,^{23, 24} exemplified by 4-(2,5-dimethyl-1H-pyrrol-1-yl)-2-hydroxybenzoic acid, which inhibit the EphA2 and EphA4 receptors;^{23,24} *iii*) doxazosin,²⁵ the marketed α_1 -adrenoreceptor antagonist that has been recently shown to bind and activate EphA2 and EphA4 receptor subtypes; *iv*) some polyphenols and polyphenol metabolites.²⁶⁻²⁸

Among these classes of Eph-ephrin system modulators, we recently focused our attention on LCA, a compound characterized by a (5 β)-cholan-24-oic acid scaffold, which competitively displaces ephrin-A1 from the ligand-binding domain of EphA2.²¹ In the present work, we report the synthesis and structure-activity relationship (SAR) profile of an extended series of α -amino acid conjugates of LCA, designed starting from a theoretical binding mode of LCA into the EphA2 binding site. The synthesized compounds were examined for their ability to disrupt EphA2-ephrin-A1 binding and to prevent EphA2 phosphorylation in a prostate cancer cell line.

CHEMISTRY

Lithocholic acid (LCA, compound **1**) was purchased from Sigma while compounds **2**, **4-7** and **12-21** were synthesized according to a procedure similar to that described in references.^{29,30} Methyl ester hydrochlorides of α -amino acids were purchased from commercial suppliers (**3a**, **4b-7b**, **12b**, **14b**, **16b-18b**, **20b**) or synthesized following step *i* of Scheme 1 (i.e. methyl ester hydrochloride derivatives **13b**, **15b**, **19b** and **21b**). The methyl

ester hydrochloride of the proper α -amino acid was reacted with **1** (LCA), using *N*-(3-dimethylaminopropyl)-*N'*-ethylcarbodiimide hydrochloride (EDCI) as coupling agent. The resulting amides **3**, **4a-7a**, **12a-21a** were hydrolyzed with NaOH to give compounds **2**, **4-7**, and **12-21**.

Compounds **8** and **9** were synthesized according to the procedure reported in Scheme 2. Methyl ester hydrochlorides **8c** and **9c** were prepared starting from *O*-benzyl L- or D-serine. Then compounds **8c** and **9c** were coupled to **1** (as described above), giving the corresponding amide conjugates **8b** and **9b**. Reductive deprotection of intermediates **8b** and **9b** afforded **8a** and **9a**. These compounds were hydrolyzed giving the final products **8** and **9**.

Compounds **10** and **11** were synthesized according to the procedure reported in Scheme 3. The amino group of L- or D-asparagine was protected with di *tert*-butyl dicarbonate (Boc₂O). This reaction gave compounds **10d** and **11d**, which were transformed in the corresponding benzyl esters **10c** and **11c**. The Boc protection was then removed giving **10b** and **11b**, which in turn were coupled to **1** to obtain compounds **10a** and **11a**.³¹ The final products **10** and **11** were obtained by removing the benzyl ester protection via hydrogenation.

RESULTS AND DISCUSSION

Molecular modeling and discovery of glycolithocholic acid (**2**) as an EphA2 antagonist

Molecular modeling investigations previously performed by our group²² suggested that LCA (**1**) can mimic the binding mode of ephrin-A1 to the EphA2 receptor³² by inserting its cyclopenta[a]perhydrophenanthrene scaffold into the hydrophobic EphA2 receptor ligand-binding channel and forming a salt bridge with Arg103 (Figure 2A), a critical residue for ephrin-A1 recognition.²⁹ In agreement with this hypothesis, modifications of the carboxylic group of LCA, e.g. esterification, led to inactive or poorly active compounds.²² However, visual inspection of the EphA2-LCA complex suggested that conjugation of LCA with natural α -amino acids, exemplified by the glycine derivative **2** (glycolithocholic acid), would lead to compounds still able to form a salt bridge with Arg103 (Figure 2B), and potentially able to undertake additional interactions with EphA2, thus endowed with higher potency than LCA.

To verify this hypothesis, we evaluated the EphA2 binding properties of compound **2** by means of an ELISA assay.²¹ A dose-dependent disruption of the EphA2-ephrin-A1 complex was observed when compound **2** was co-incubated with these two proteins (Figure 3A). Compound **2** had pIC₅₀ (-log (IC₅₀)) of 4.31, similar to the value previously found for LCA. To evaluate the nature of the antagonism of compound **2**, saturation curves of EphA2-ephrin-A1 binding in the presence of increasing concentrations of compound **2** were plotted (Figure 3B). From each of these curves, the K_D or the apparent K_D values were calculated and the corresponding Schild plot was generated (Figure 3C). The slope of the regression line of the Schild plot was 1.35 units ($r^2 = 0.97$), indicating competitive binding of compound **2** to the EphA2 receptor. The displacement experiment was repeated by incubating 100 μ M of compound **2** for 1 hour and washing some wells before adding 50 ng/mL ephrin-A1-Fc. The displacement was detected only where the washing was not performed, suggesting that compound **2** acts as reversible binder of the EphA2 receptor (Figure 3D).

Structure-activity relationship (SAR) analysis of LCA derivatives

Based on the results reported above, we decided to synthesize an extended set of α -amino acid derivatives of LCA (**3-21**). Compounds **3-21** were evaluated for their ability to disrupt

the binding of ephrin-A1 to the EphA2 receptor, using the ELISA binding protocol described above.²¹ The pIC₅₀ values for the different compounds are reported in Table 1, together with the corresponding standard deviations of the mean (SEM).

We began our investigation by comparing the activity of compounds **1-3** in the binding assay. Compounds **1** and **2** were both active in preventing the binding of ephrin-A1 to EphA2, with pIC₅₀ values of 4.20 and 4.31, respectively. Conversely, compound **3**, the methyl ester derivative of **2**, resulted inactive, confirming the importance of a free carboxyl group for maintaining biological activity. We next synthesized and tested eight α -amino acid conjugates (**4-11**), the side chains of which (L- and D-Ala, L- and D-Ser, L- and D-Val, L- and D-Asn) represent the four combinations of positive and negative levels for lipophilicity and steric hindrance, as described by π and MR (molar refractivity) variables, respectively (Figure 4).

pIC₅₀ Values for these compounds indicated that the hydrophobic groups (**4-7**) had a favorable impact on potency, regardless of the absolute configuration of the chiral centre on the amino acid moiety. On the other hand, the introduction of hydrophilic groups was tolerated for the small side chains of serine derivatives (**8,9**) but it was detrimental for activity in the case of the bulkier side chain of asparagine (**10,11**). Ten additional α -amino acids were then coupled with LCA, to further cover the space of lipophilic and steric properties. We confirmed the negative effect of polar amino side chains synthesizing L- and D-Asp derivatives (**12, 13**) which proved to be inactive. On the other hand, the introduction of amino acids with lipophilic side chains always led to active compounds. Compounds **14** and **15**, bearing a methionine side chain, showed a limited increment in the binding activity compared to compound **1**. Notably, the introduction of aromatic substituents had a significant impact on pIC₅₀. Phenylalanine derivatives **16** and **17** resulted nearly ten times more potent than LCA. Conversely, the replacement of phenylalanine with tyrosine led to poorly active compounds (**18, 19**) possibly due to their lower lipophilicity. The importance of a lipophilic group at the α position was further confirmed by the tryptophan conjugates **20** and **21**, which were significantly more active than LCA. In particular, the L-Trp conjugate **20** showed a pIC₅₀ of 5.69, resulting the most potent EphA2 ligand of the series.

As the amino acid side chains of compounds **2** and **4-21** constitute a set with a large variation in both lipophilicity (almost 2 π units) and steric bulk (40 MR units), we examined the statistical relationship between these properties and the pIC₅₀ values. A poor correlation was found for pIC₅₀ with π ($r^2 = 0.29$) as well as with the steric descriptor MR ($r^2 = 0.22$). Therefore, while it could be qualitatively inferred that hydrophobic interactions are crucial for potent ligands, side chain lipophilicity (π) appears inadequate to quantitatively explain the variation in potency.

The availability of the X-ray crystal structure of EphA2 in complex with the ephrin-A1 ligand³⁴ prompted us to evaluate the existence of a correlation between experimental pIC₅₀ and free energy of binding estimated by means of theoretical methods. Compounds **2, 4-9** and **14-21** were docked into the EphA2 binding site using the Glide software³⁵ and then, for each of the resulting protein-ligand complexes, the binding free energy was estimated using the MM-GBSA approach³⁶ implemented in Prime,³⁷ and the MM-PBSA approach³⁸ implemented in Impact.³⁹

These methods employ a combination of molecular mechanics and continuum solvation to elicit binding free energy directly from structural information at a reasonable computational cost. MM-GBSA is becoming a standard tool to rescore docking poses in the field of structure-based drug design. Indeed, it provided improved enrichment in virtual screening of databases and superior correlation between calculated binding affinities and experimental

data in lead optimization of sets of congeneric inhibitors when compared to classical scoring function.⁴⁰

The docking approach applied here gave binding poses for the synthesized compounds superimposable to that of glycolithocholic acid **2** (Figure 2B). The resulting complexes highlighted the presence of an accessory hydrophobic site in the ligand-binding channel of the EphA2 receptor where the α -side chain of the conjugated derivatives could be accommodated. Such a binding mode can thus explain the lack of activity for the more polar derivatives **10-13**, as well as the significant increment in the pIC₅₀ values observed for the aromatic derivatives **16, 17, 20**, and **21** bearing a phenylalanine or a tryptophan portion. Visual inspection of the EphA2-compound **20** complex further supported the importance of aromatic interactions at the EphA2 receptor (Figure 5). Indeed the indole ring of **20** tightly interacts with Phe108, a conserved residue responsible for the recognition of one of the two aromatic residues (namely Phe111) of the ϕ -x-x- ϕ binding motif of ephrin ligands.^{41,42} Superposition of ephrin-A1, co-crystallized with EphA2, and compound **20** docked into the same receptor (Figure 5), shows that the binding mode proposed for this compound closely resembles the arrangement of the protein ligand at its binding site.

Despite the qualitative rationalization of the SAR data provided by these molecular models, no correlation was found between the Glide score and the experimental pIC₅₀ (data not shown). To search for a better correlation between experimental and calculated pIC₅₀ values, MM-GBSA and MM-PBSA energies were calculated for EphA2-ligand complexes. Linear regression gave $r^2 = 0.68$ with MM-GBSA ($n = 15$, $s = 0.25$, $F = 26$) and $r^2 = 0.65$ with MM-PBSA ($n = 15$, $s = 0.26$, $F = 23$). The MM-GBSA model accounts for the introduction of bulky groups at the α -position of the amino acid portion as well as for the difference in pIC₅₀ values between the two tryptophan-based stereoisomers **20** and **21** on the ΔG scale (Figure 6). On the other hand, the MM-GBSA approach was not fully able to capture the detrimental effects on activity observed when the phenylalanine portion of **16** and **17** was replaced by a tyrosine in compounds **18** and **19**. Similar indications were obtained from the MM-PBSA regression model (Figure S1).

Despite this limitation, the MM-GBSA and MM-PBSA binding energy values outperformed classical property descriptors, such as π or MR, in rationalizing SAR data. All these findings indicate that strict stereoelectronic complementarity between EphA2 and LCA conjugates is fundamental to achieve high pIC₅₀ values.

Selectivity profile of compound **20**

We further examined the ability of L-Trp derivative **20** to inhibit ephrin binding to all EphA and EphB receptors by using biotinylated ephrin-A1-Fc and biotinylated ephrin-B1-Fc, respectively, at their K_D concentration (see Experimental Section).

Similar to lithocholic acid,²¹ compound **20** was able to inhibit ephrin binding to all members of the Eph receptor family (Figure 7). A moderate selectivity towards EphA receptors was however observed. Indeed, compound **20** showed IC₅₀ values in the low μ M range for all EphA and EphB receptors. This suggests that compound **20** interferes with Eph receptor-ephrin recognition by occupying a highly conserved region within the Eph receptor ligand binding domain (Figure 5).

Effects on EphA2 phosphorylation in human prostate adenocarcinoma cells

LCA conjugates with L-amino acids (i.e. compounds **4,6,8,14,16,20**) had slightly higher pIC₅₀ values than those resulting from conjugation with the corresponding D-amino acids (i.e. compounds **5,7,9,15,17,21**) in the ELISA binding assay. We thus focused our attention

on the first sub-class of LCA conjugates for functional investigations. To evaluate the functional effects of **4**, **6**, **8**, **14**, **16** and **20**, we performed phosphorylation studies using PC3 human prostate adenocarcinoma cells, which predominantly express the EphA2 receptor.⁴³ Glycolithocholic acid **2** was also included as a reference compound. All the tested compounds were unable to stimulate EphA2 tyrosine phosphorylation on their own (data not shown), but behaved as pure antagonists of the EphA2 receptor, inhibiting EphA2 phosphorylation induced by ephrin-A1-Fc in a dose-dependent manner (Figure 8).

The L-Phe and L-Trp conjugates **16** and **20** inhibited EphA2 phosphorylation with IC₅₀ values of 19 and 12 μM, emerging as the most potent antagonists of the series. In particular, compound **20** resulted 5-10 times more potent than **1** (LCA; IC₅₀ = 50 μM)²¹ and **2** (IC₅₀ = 138 μM) in blocking EphA2 phosphorylation in PC3 cell line.

Finally, pIC₅₀ values of **2**, **4**, **6**, **8**, **14**, **16** and **20** measured in the phosphorylation assay roughly paralleled the pIC₅₀ ones obtained in the EphA2-binding assays ($r^2 = 0.77$, Figure 9), confirming that compounds having higher potency in EphA2 binding were also more effective in preventing EphA2 activation.

Effect on morphology in human prostate adenocarcinoma cells

Activation of EphA2 is known to induce important changes in cell morphology, such as retraction of the cell periphery and rounding. Rounding and retraction are critical cellular responses that being responsible for cell migration are directly correlated to cancer cell invasiveness as well as to formation of new vessels by endothelial cells.⁴⁴ To evaluate whether small molecule antagonists of the EphA2 receptor can effectively block cell rounding and retraction, we tested compound **20** on PC3 prostate cancer cells, which predominantly express the EphA2 receptor.⁴³

In good agreement with the inhibitory effect shown on EphA2 phosphorylation (Figure 8), treatment with compound **20** dose-dependently reduced (IC₅₀ = 5.1 μM) the percentage of retracted cells due to ephrin-A1-Fc stimulation (Figure 10). This indicates that compound **20** can be effectively used to counteract the functional effects mediated by EphA2. Finally, compound **20** did not affect cell morphology in the absence of ephrin treatment, nor had cytotoxic effect on PC3 cells at the tested concentrations, as shown in an LDH assay (Figure S2).

CONCLUSIONS

Increasing evidence supports the notion that the Eph–ephrin system, including the EphA2 receptor, plays a critical role in tumor vascularization during carcinogenesis. In particular, EphA2 is currently being explored as a novel target for the development of anti-tumorigenic and anti-angiogenic therapies.

Few classes of small molecules able to bind the EphA2 receptor have been recently discovered and employed for biological investigations. However, their usefulness as biological tools seems limited by pharmacological and/or chemical issues. For instance, doxazosin, an α₁-adrenergic receptor blocker, binds the EphA2 receptor with low affinity²⁵ and chemical stability concerns have been raised for EphA2/EphA4 salicylic acid antagonists. These compounds undergo a modification process that leads to the formation of an unidentified molecular entity able to interact with Eph receptors.^{23,45} In this context, it is critical to search for new compounds able to bind the EphA2 receptor with better chemical and pharmacological profiles.

In the present study, a computationally-driven exploration of LCA analogues led us to synthesize a series of α -amino acid conjugates. As a result of the SAR investigation, we identified the L-Trp conjugated of LCA, **20**, (PCM126) as the most potent derivative. Compound **20** disrupts EphA2-ephrin-A1 interaction at low micromolar concentrations ($pIC_{50} = 5.69$) preventing EphA2 activation and cell retraction in human prostate adenocarcinoma cells with similar antagonist potency. Compound **20** therefore represents one the most potent non-peptide antagonist of the EphA2 receptor. Other small-molecule antagonists of EphA2, i.e. the reference compound 4-(2,5-dimethyl-1H-pyrrol-1-yl)-2-hydroxybenzoic acid, only block EphA2 activity in cells at very high concentrations,²⁴ while preventing the binding of ephrin ligands at low micromolar concentrations in ELISA assays.

Due to the presence of the bile-acid scaffold, compound **20** possesses critical physicochemical properties and potential off target activities^{46,47} that might hamper its application *in vivo*. However, this compound can be used as a pharmacological tool to assess the potential of pharmacological therapy based on small molecule Eph antagonists, as well as a starting point to design more potent antagonists of the EphA2 receptor with improved drug-like profile.

EXPERIMENTAL SECTION

Molecular Modelling

Docking simulations—Molecular modelling simulations were performed starting from the crystal structure of the EphA2-ephrin-A1 complex (3HEI.pdb),³⁴ using Maestro software⁴⁸ and OPLS2005 force field.⁴⁹ The EphA2-ephrin-A1 complex was submitted to a protein preparation procedure. Molecular models of compounds **1-2**, **4-21** were built using Maestro, and their geometry optimized by energy minimization using OPLS2005 to a energy gradient of 0.01 kcal/(mol · Å). Docking simulations were performed using Glide5.5, starting from the minimized structure of the compounds placed in an arbitrary position within a region centered on the surface of channel of EphA2, delimited by Arg103, Phe156 and Arg159, using enclosing and bounding boxes of 20 and 14 Å on each side, respectively. Van der Waals radii of the protein atoms were not scaled, while van der Waals radii of the ligand atoms with partial atomic charges lower than $|0.15|$ were scaled by 0.8. Extra precision (XP) mode was applied. The resulting binding poses were ranked according to the Gscore, and the best docking solution for each compound was selected for MM-GBSA calculations.

MM-GBSA and MM-PBSA calculations—Although MM-GBSA and MM-PBSA are typically applied to large collections of equilibrated structures of protein-ligand complexes sampled during molecular dynamics in water, these methods can give a reasonable estimation of the ligand affinity also employing a single energy-minimized structure as reported in literature.^{38,40}

Specifically MM-GBSA calculations were performed as follow: the docked poses generated with Glide5.5 were minimized using the local optimization feature in Prime, and the energies were calculated using the OPLS2005 force field and the GBSA continuum model in Maestro.⁴⁸ The free energy of binding was then estimated by applying the MM-GBSA method as implemented in Prime.^{36,40} With this approach, the binding free energy ΔG_{bind} is estimated as:

$$\Delta G_{\text{bind}} = \Delta E_{\text{MM}} + \Delta G_{\text{solv}} + \Delta G_{\text{SA}}$$

where ΔE_{MM} is the difference in energy between the complex structure and the sum of the energies of the ligand and free protein, using the OPLS force field; ΔG_{solv} is the difference in the GBSA solvation energy of the complex and the sum of the solvation energies for the ligand and unliganded protein, and ΔG_{SA} is the difference in the surface area energy for the complex and the sum of the surface area energies for the ligand and uncomplexed protein. Corrections for entropic changes were not applied.

The free energy of binding was then estimated by applying the MM-PBSA method in combination with energy minimization using Impact software³⁹ starting from the MM-GBSA energy minima of the EphA2-ligand complexes. Standard settings of Impact, as implemented in Maestro,⁴⁸ were employed.

Chemistry

Unless otherwise noted, reagents and solvents were purchased from commercial suppliers (Aldrich and Fluka) and were used without purification. The progress of the reactions was monitored by thin-layer chromatography with F254 silica-gel pre-coated sheets (Merck Darmstadt, Germany). Flash chromatography was performed using Merck silica-gel 60 (Si 60, 40-63 μm , 230-400 mesh ASTM). Catalytic hydrogenation was performed using a Parr 3911 Hydrogenation apparatus. Melting points were determined on a Gallenkamp melting point apparatus and were not corrected. The $^1\text{H-NMR}$ and $^{13}\text{C-NMR}$ spectra were recorded on a Bruker Avance 400 spectrometer (400MHz). Mass spectra were recorded on an Applied Biosystem API-150 EX system spectrometer with ESI interface. The final compounds were analyzed on a ThermoQuest (Italia) FlashEA 1112 Elemental Analyzer for C, H and N. The percentages found were within $\pm 0.4\%$ of the theoretical values. All the tested compounds were $>95\%$ pure as determined by elemental analysis. Characterization data, including mp, $^1\text{H-NMR}$ and $^{13}\text{C-NMR}$, MS data, and the results of elemental analysis, are available as Supporting Information.

With the exception of **2**,³⁰ **3**,⁵⁰ **12**³⁰ and **20**,⁵¹ all the other synthesized compounds are reported here for the first time.

Pharmacology

Reagents—All culture media and supplements were purchased from Lonza. Recombinant proteins and antibodies were from R&D systems. Cells were purchased from ECACC. Leupeptin, aprotinin, NP40, tween20, BSA and salts for solutions were from Applichem; EDTA and sodium orthovanadate were from Sigma. Human IgG Fc fragment was from Millipore (AG714).

Cell Cultures—PC3 human prostate adenocarcinoma cells were grown in RPMI-1640 media and supplemented with 7% fetal bovine serum (FBS) and 1% antibiotic solution. PC3 were grown in a humidified atmosphere of 95% air, 5% CO_2 at 37°C.

ELISA assays and K_i /IC₅₀ determination—ELISA assays were performed as previously described.²¹ Briefly, compounds were stocked as 20 mM solutions in dimethyl sulfoxide (DMSO) and tested in displacing studies, starting from a concentration of 100 μM . Ninety-six well ELISA high binding plates (Costar #2592) were incubated overnight at 4 °C with 100 μL /well of 1 $\mu\text{g}/\text{mL}$ EphA2-Fc (R&D 639-A2) diluted in sterile phosphate buffered saline (PBS, 0.2 g/L KCl, 8.0 g/L NaCl, 0.2KH₂PO₄, 1.15 g/L Na₂HPO₄, pH 7.4). The day after wells were washed with washing buffer (PBS +0.05% tween20, pH 7.5) and blocked with blocking solution (PBS +0.5% BSA) for 1 h at 37 °C. Compounds were added to the wells at proper concentration in 1% DMSO and incubated at 37 °C for 1 h. Biotinylated ephrin-A1-Fc (R&D Systems BT602) was added at 37 °C for 4 hours at its K_D

in displacement assays or in a range from 1 to 2000 ng/ml in saturation studies. The wells were washed and incubated with 100 μ l/well Streptavidin-HRP (Sigma S5512) in blocking solution (0.05 μ g/mL in PBS supplemented with 0.5% BSA, pH 7.4) for 20 minutes at room temperature, then washed again and incubated at room temperature with 0.1 mg/mL tetramethylbenzidine (Sigma T2885) reconstituted in stable peroxide buffer (11.3 g/L citric acid, 9.7 g/L sodium phosphate, pH 5.0) and 0.02% H₂O₂ (30% m/m in water), added immediately before use. The reaction was stopped with 3N HCl 100 μ L/well and the absorbance was measured using an ELISA plate reader (Sunrise, TECAN, Switzerland) at 450 nm. IC₅₀ values were determined using one-site competition non-linear regression analysis with Prism software (GraphPad Software Inc.). During the experiment to determine selectivity of compounds, all EphAs (R&D Systems SMPK1) and EphBs (R&D Systems SMPK2) receptors were incubated overnight similarly to EphA2 as previously described; 150 ng/ml biotinylated ephrin-A1-Fc or biotinylated ephrin-B1-Fc (R&D Systems BT473) was used with EphAs or EphBs, respectively.

Phosphorylation of EphA2 in cells—PC3 cells were seeded in 12-well plates at concentration of 105 cells/ml, 1 ml/well, in complete medium until they reached ~70% confluence and serum starved overnight. The day after cells were treated with the compounds under study, vehicle or standard drug, stimulated with ephrin-A1-Fc, rinsed with sterile PBS and solubilized in lysis buffer (1% NP-40, 20 mM Tris (pH 8.0), 137 mM NaCl, 10% glycerol, 2 mM EDTA, 1 mM activated sodium orthovanadate, 10 μ g/mL Aprotinin, 10 μ g/mL Leupeptin). The lysates were resuspended and rocked at 4 °C for 30 minutes and then centrifuged at 14000 \times g for 5 minutes. The protein content of supernatant was measured with BCA protein assay kit (Thermo scientific) and standardized to 200 μ g/mL.

EphA2 phosphorylation was measured in cell lysates using a DuoSet®IC Sandwich ELISA (R&D Systems, #DYC4056) following the manufacturer's protocol. Briefly, 96 well ELISA high binding plates (costar 2592) were incubated overnight at room temperature with 100 μ L/well of EphA2 capture antibody diluted in sterile PBS to the proper working concentration. After blocking, the wells were incubated for 2 h at room temperature with 100 μ L/well of lysates, followed by a 2 h incubation at room temperature with the detection antibody. Receptor phosphorylation was revealed utilizing a standard HRP format with a colorimetric reaction read at 450 nm.

LDH assay—Cytotoxicity of compound **20** was evaluated with CytoTox 96® Non-Radioactive Cytotoxicity Assay, following the manufacturer's protocol (Promega, #1780). Briefly, cells were seeded in 96-well plates at a density of 10⁵ cells/ml and the day after treated with compounds or lysis buffer for 2h. After incubation, released LDH in culture supernatants was measured using a 30-minute coupled enzymatic assay, which results in conversion of a tetrazolium salt (INT) into a red formazan product. The amount of colour formed is proportional to the number of lysed cells and quantified by ELISA plate reader (Sunrise, TECAN, Switzerland) at 492 nm. The results were expressed as the ratio between absorbance of the cells treated with the compounds and cells treated with lysis buffer.

Retraction assay—The procedure is similar to that reported in references 21 and 22. Briefly, PC3 cells (4,000 cells per well) were plated in 96-well plates (Greiner Bio One, Frickenhausen Germany) and grown for 17 hours. The cells were starved for 1 hour in serum-free RPMI, incubated for 15 min with the compounds or DMSO, and stimulated for 10 min with 0.5 μ g / ml ephrin-A1 Fc or Fc as a control. The cells were then fixed for 15 min in 4% formaldehyde in PBS, permeabilized for 3 min in 0.5% Triton X-100 in TBS, and stained with rhodamine-conjugated phalloidin (Invitrogen). Nuclei were labeled with 4',6-diamidino-2-phenylindole (DAPI). Cells were photographed under a fluorescence microscope, and the number of retracted cells was counted in a blinded manner.

Supplementary Material

Refer to Web version on PubMed Central for supplementary material.

Acknowledgments

The authors thank Dr. Caterina Carmi (Università degli Studi di Parma) for critical reading of the manuscript. Prof. Amedeo Caflisch (Department of Biochemistry, University of Zurich) is also acknowledged for useful discussions. This work was supported by Ministero dell'Università e della Ricerca, "Futuro in Ricerca" program (project code: RBFR10FXCP), My First AIRC Grant (MFAG 6181) and grant CA138390 from the National Institutes of Health. I.H.M thanks the Italian Society of Pharmacology (SIF) for supporting the permanence at the Sanford-Burnham Medical Research Institute.

ABBREVIATIONS USED

ATP	adenosine triphosphate
ELISA	enzyme linked immunosorbent assay
EDCI	N-(3-dimethylaminopropyl)-N'-ethylcarbodiimide hydrochloride
LCA	lithocholic acid
Eph	erythropoietin-producing hepatocellular carcinoma
MM-GBSA	Molecular Mechanics/Generalized Born Surface Area
NMM	N-methyl morpholine
PBS	phosphate buffered saline
SAR	structure–activity relationship
TK	tyrosine kinase

REFERENCES

1. Gale NW, Yancopoulos GD. Ephrins and their receptors: a repulsive topic? *Cell Tissue Res.* 1997; 290:227–241. [PubMed: 9321684]
2. Himanen JP, Saha N, Nikolov DB. Cell-cell signaling via Eph receptors and ephrins. *Curr. Opin. Cell. Biol.* 2007; 19:534–542. [PubMed: 17928214]
3. Pasquale EB. Eph receptor signalling casts a wide net on cell behaviour. *Nat. Rev. Mol. Cell. Biol.* 2005; 6:462–475. [PubMed: 15928710]
4. Prevost N, Woulfe D, Tognolini M, Brass LF. Contact-dependent signaling during the late events of platelet activation. *J. Thromb. Haemost.* 2003; 1:1613–1627. [PubMed: 12871298]
5. Pasquale EB. Eph-ephrin bidirectional signaling in physiology and disease. *Cell.* 2008; 133:38–52. [PubMed: 18394988]
6. Pasquale EB. Eph receptors and ephrins in cancer: bidirectional signalling and beyond. *Nat. Rev. Cancer.* 2010; 10:165–180. [PubMed: 20179713]
7. Brantley-Sieders DM. Clinical relevance of Ephs and ephrins in cancer: lessons from breast, colorectal, and lung cancer profiling. *Semin. Cell. Dev. Biol.* 2012; 23:102–108. [PubMed: 22040912]
8. Beauchamp A, Debinski W. Ephs and ephrins in cancer: ephrin-A1 signalling. *Semin. Cell. Dev. Biol.* 2012; 23:109–115. [PubMed: 22040911]
9. Merlos-Suarez A, Batlle E. Eph-ephrin signalling in adult tissues and cancer. *Curr. Opin. Cell. Biol.* 2008; 20:194–200. [PubMed: 18353626]
10. Noren NK, Pasquale EB. Paradoxes of the EphB4 receptor in cancer. *Cancer Res.* 2007; 67:3994–3997. [PubMed: 17483308]

11. Kuijper S, Turner CJ, Adams RH. Regulation of angiogenesis by Eph-ephrin interactions. *Trends Cardiovasc. Med.* 2007; 17:145–151. [PubMed: 17574121]
12. Martiny-Baron G, Holzer P, Billy E, Schnell C, Brueggen J, Ferretti M, Schmiedeberg N, Wood JM, Furet P, Imbach P. The small molecule specific EphB4 kinase inhibitor NVP-BHG712 inhibits VEGF driven angiogenesis. *Angiogenesis.* 2010; 13:259–267. [PubMed: 20803239]
13. Wang S, Placzek WJ, Stebbins JL, Mitra S, Noberini R, Koolpe M, Zhang Z, Dahl R, Pasquale EB, Pellecchia M. Novel targeted system to deliver chemotherapeutic drugs to EphA2-expressing cancer cells. *J. Med. Chem.* 2012; 55:2427–2436. [PubMed: 22329578]
14. Tandon M, Vemula SV, Mittal SK. Emerging strategies for EphA2 receptor targeting for cancer therapeutics. *Expert Opin. Ther. Targets.* 2011; 15:31–51. [PubMed: 21142802]
15. Lafleur K, Huang D, Zhou T, Caflisch A, Nevado C. Structure-based optimization of potent and selective inhibitors of the tyrosine kinase erythropoietin producing human hepatocellular carcinoma receptor B4 (EphB4). *J. Med. Chem.* 2009; 52:6433–6446. [PubMed: 19788238]
16. Mamat C, Mosch B, Neuber C, Kockerling M, Bergmann R, Pietzsch J. Fluorine-18 Radiolabeling and Radiopharmacological Characterization of a Benzodioxolylpyrimidine-based Radiotracer Targeting the Receptor Tyrosine Kinase EphB4. *ChemMedChem.* 2012 doi: 10.1002/cmde.201200264.
17. van Linden OP, Farenc C, Zoutman WH, Hameetman L, Wijtmans M, Leurs R, Tensen CP, Siegal G, de Esch IJ. Fragment based lead discovery of small molecule inhibitors for the EPHA4 receptor tyrosine kinase. *Eur. J. Med. Chem.* 2012; 47:493–500. [PubMed: 22137457]
18. Noberini R, Lamberto I, Pasquale EB. Targeting Eph receptors with peptides and small molecules: progress and challenges. *Semin. Cell. Dev. Biol.* 2012; 23:51–7. [PubMed: 22044885]
19. Wells JA, McClendon CL. Reaching for high-hanging fruit in drug discovery at protein-protein interfaces. *Nature.* 2007; 450:1001–1009. [PubMed: 18075579]
20. Jehle J, Staudacher I, Wiedmann F, Schweizer PA, Becker R, Katus HA, Thomas D. Regulation of HL-1 cardiomyocyte apoptosis by EphA2 receptor tyrosine kinase phosphorylation and protection by lithocholic acid. *Br. J. Pharmacol.* 2012; 167:1563–1572. [PubMed: 22845314]
21. Giorgio C, Hassan Mohamed I, Flammini L, Barocelli E, Incerti M, Lodola A, Tognolini M. Lithocholic acid is an Eph-ephrin ligand interfering with Eph-kinase activation. *PLoS One.* 2011; 6:e18128. [PubMed: 21479221]
22. Tognolini M, Incerti M, Hassan-Mohamed I, Giorgio C, Russo S, Bruni R, Lelli B, Bracci L, Noberini R, Pasquale EB, Barocelli E, Vicini P, Mor M, Lodola A. Structure-activity relationships and mechanism of action of Eph-ephrin antagonists: interaction of cholanic acid with the EphA2 receptor. *ChemMedChem.* 2012; 7:1071–1083. [PubMed: 22529030]
23. Noberini R, De SK, Zhang Z, Wu B, Raveendra-Panickar D, Chen V, Vazquez J, Qin H, Song J, Cosford ND, Pellecchia M, Pasquale EB. A disalicylic acid-furanyl derivative inhibits ephrin binding to a subset of Eph receptors. *Chem. Biol. Drug Des.* 2011; 78:667–678. [PubMed: 21791013]
24. Noberini R, Koolpe M, Peddibhotla S, Dahl R, Su Y, Cosford ND, Roth GP, Pasquale EB. Small molecules can selectively inhibit ephrin binding to the EphA4 and EphA2 receptors. *J. Biol. Chem.* 2008; 283:29461–29472. [PubMed: 18728010]
25. Petty A, Myshkin E, Qin H, Guo H, Miao H, Tochtrop GP, Hsieh JT, Page P, Liu L, Lindner DJ, Acharya C, Mackerell AD Jr, Ficker E, Song J, Wang B. A Small Molecule Agonist of EphA2 Receptor Tyrosine Kinase Inhibits Tumor Cell Migration In Vitro and Prostate Cancer Metastasis In Vivo. *PLoS One.* 2012; 7:e42120. [PubMed: 22916121]
26. Tognolini M, Giorgio C, Hassan Mohamed I, Barocelli E, Calani L, Reynaud E, Dangles O, Borges G, Crozier A, Brighenti F, Del Rio D. Perturbation of the EphA2-EphrinA1 System in Human Prostate Cancer Cells by Colonic (Poly)phenol Catabolites. *J. Agric. Food Chem.* 2012; 60:8877–8884. [PubMed: 22409255]
27. Noberini R, Koolpe M, Lamberto I, Pasquale EB. Inhibition of Eph receptor-ephrin ligand interaction by tea polyphenols. *Pharmacol. Res.* 2012; 66:363–373. [PubMed: 22750215]
28. Mohamed IH, Giorgio C, Bruni R, Flammini L, Barocelli E, Rossi D, Domenichini G, Poli F, Tognolini M. Polyphenol rich botanicals used as food supplements interfere with EphA2-ephrinA1 system. *Pharmacol. Res.* 2011; 64:464–470. [PubMed: 21742039]

29. Pfeffer FM, Russell RA. Strategies and methods for the attachment of amino acids and peptides to chiral [n]polynorborene templates. *Org. Biomol. Chem.* 2003; 1:1845–1851. [PubMed: 12945763]
30. Chang KH, Lee L, Chen J, Li WS. Lithocholic acid analogues, new and potent alpha-2,3-sialyltransferase inhibitors. *Chem. Commun. (Camb).* 2006:629–631. [PubMed: 16446832]
31. Wu J, Li C, Zhao M, Wang W, Wang Y, Peng S. A class of novel carboline intercalators: Their synthesis, in vitro anti-proliferation, in vivo anti-tumor action, and 3D QSAR analysis. *Bioorg. Med. Chem.* 2010; 18:6220–6229. [PubMed: 20692841]
32. Himanen JP. Ectodomain structures of Eph receptors. *Semin. Cell. Dev. Biol.* 2012; 23:35–42. [PubMed: 22044883]
33. (MOE). M. o. e. Molecular operating environment (MOE). CCG Inc; University St, Montreal, Quebec, Canada: 2008. p. 1255MOE 2008.10
34. Himanen JP, Goldgur Y, Miao H, Myshkin E, Guo H, Buck M, Nguyen M, Rajashankar KR, Wang B, Nikolov DB. Ligand recognition by A-class Eph receptors: crystal structures of the EphA2 ligand-binding domain and the EphA2/ephrin-A1 complex. *EMBO Rep.* 2009; 10:722–728. [PubMed: 19525919]
35. Glide. Schrodinger LLC; N. Y., NY: 2009. 5.5
36. Lyne PD, Lamb ML, Saeh JC. Accurate prediction of the relative potencies of members of a series of kinase inhibitors using molecular docking and MM-GBSA scoring. *J. Med. Chem.* 2006; 49:4805–4808. [PubMed: 16884290]
37. Prime. Schrodinger LLC; N. Y., NY: 2009. 3.0
38. Rastelli G, Del Rio A, Degliesposti G, Sgobba M. Fast and accurate predictions of binding free energies using MM-PBSA and MM-GBSA. *J. Comput. Chem.* 2010; 31:797–810. [PubMed: 19569205]
39. Impact. Schrodinger LLC; N. Y., NY: 2009. 5.8
40. Guimaraes CR, Cardozo M. MM-GB/SA rescoring of docking poses in structure-based lead optimization. *J. Chem. Inf. Model.* 2008; 48:958–970. [PubMed: 18422307]
41. Lema Tome CM, Palma E, Ferluga S, Lowther WT, Hantgan R, Wykosky J, Debinski W. Structural and functional characterization of monomeric EphrinA1 binding site to EphA2 receptor. *J. Biol. Chem.* 2012; 287:14012–14022. [PubMed: 22362770]
42. Koolpe M, Dail M, Pasquale EB. An ephrin mimetic peptide that selectively targets the EphA2 receptor. *J. Biol. Chem.* 2002; 277:46974–94697. [PubMed: 12351647]
43. Noberini R, Rubio de la Torre E, Pasquale EB. Profiling Eph receptor expression in cells and tissues: a targeted mass spectrometry approach. *Cell. Adh. Migr.* 2012; 6:102–112. [PubMed: 22568954]
44. Miao H, Burnett E, Kinch M, Simon E, Wang B. Activation of EphA2 kinase suppresses integrin function and causes focal-adhesion-kinase dephosphorylation. *Nat. Cell. Biol.* 2000; 2:62–69. [PubMed: 10655584]
45. Baell JB, Holloway GA. New substructure filters for removal of pan assay interference compounds (PAINS) from screening libraries and for their exclusion in bioassays. *J. Med. Chem.* 2010; 53:2719–2740. [PubMed: 20131845]
46. Pellicciari R, Gioiello A, Macchiarulo A, Thomas C, Rosatelli E, Natalini B, Sardella R, Pruzanski M, Roda A, Pastorini E, Schoonjans K, Auwerx J. Discovery of 6alpha-ethyl-23(S)-methylcholic acid (S-EMCA, INT-777) as a potent and selective agonist for the TGR5 receptor, a novel target for diabetes. *J. Med. Chem.* 2009; 52:7958–7961. [PubMed: 20014870]
47. Pellicciari R, Costantino G, Camaioni E, Sadeghpour BM, Entrena A, Willson TM, Fiorucci S, Clerici C, Gioiello A. Bile acid derivatives as ligands of the farnesoid X receptor. Synthesis, evaluation, and structure-activity relationship of a series of body and side chain modified analogues of chenodeoxycholic acid. *J. Med. Chem.* 2004; 47:4559–4569. [PubMed: 15317466]
48. Maestro. Schrodinger LLC; N. Y., NY: 2009. 9.0
49. Jorgensen WL, Maxwell DS, Tirado-Rives J. Development and testing of the OPLS all-atom force field on conformational energetics and properties of organic liquids. *J Am Chem Soc.* 1996; 118:11225–11236.

50. Bolt MJ. Separation of methylated free bile acids from their taurine and methyl glycine conjugates by thin-layer chromatography. *J. Lipid Res.* 1987; 28:1013–1015. [PubMed: 2444665]
51. Jacobson AR, Gabler DG, Oleksyszyn J. Bile acid inhibitors of metalloproteinase enzymes. 1997 Patent US005646316A.

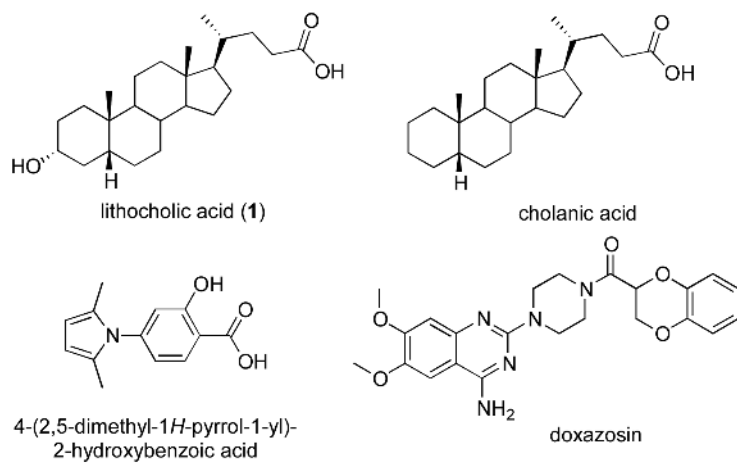


Figure 1.
Low-molecular weight modulators of the Eph receptor family.

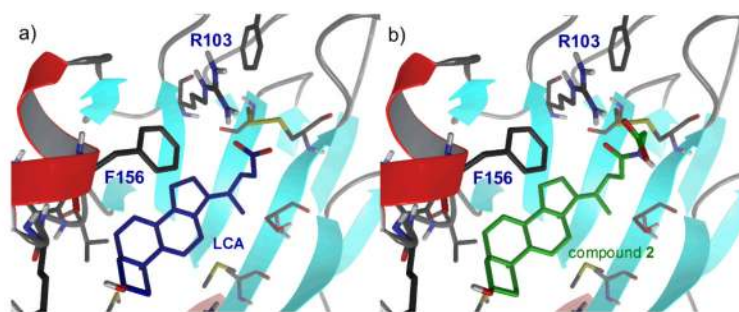


Figure 2. Lithocholic acid (panel A, blue carbon atoms) and its glyco-conjugate compound 2 (panel B, green carbon atoms) within the ligand binding domain of EphA2 receptor. Protein carbon atoms are depicted in black. Secondary structure elements of the EphA2 receptor are colored in cyan (β -sheets) and in red (α -helices).

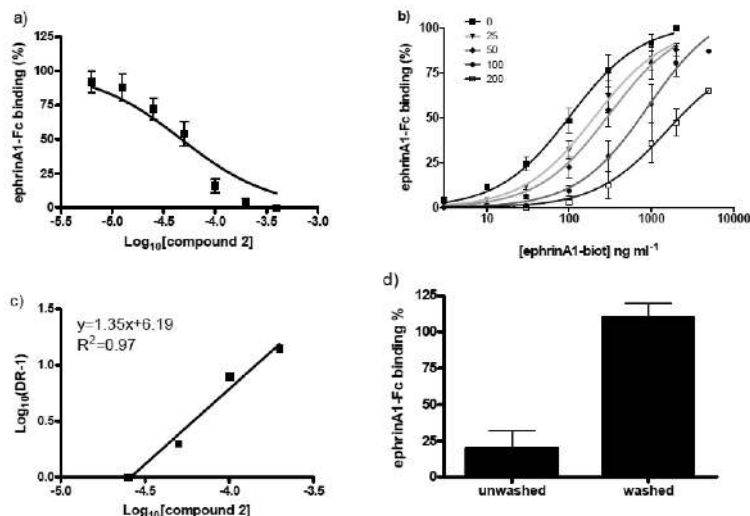


Figure 3. Compound 2 competitively inhibits EphA2-ephrin-A1 binding. A) compound 2 dose-dependently displaced binding of ephrin-A1-Fc from immobilized EphA2-Fc. B) binding of ephrin-A1-Fc to immobilized EphA2-Fc in the presence of different concentrations of compound 2. C) Dissociation constants (K_d) from the previous experiments were used to calculate $\text{Log}_{10}(\text{DR} - 1)$ and to graph the Schild plot. The $\text{p}K_i$ value for compound 2 was estimated by the intersection of the interpolated line with the X-axis. D) EphA2-ephrin-A1 binding in presence of 100 μM compound 2, with or without washing with PBS.

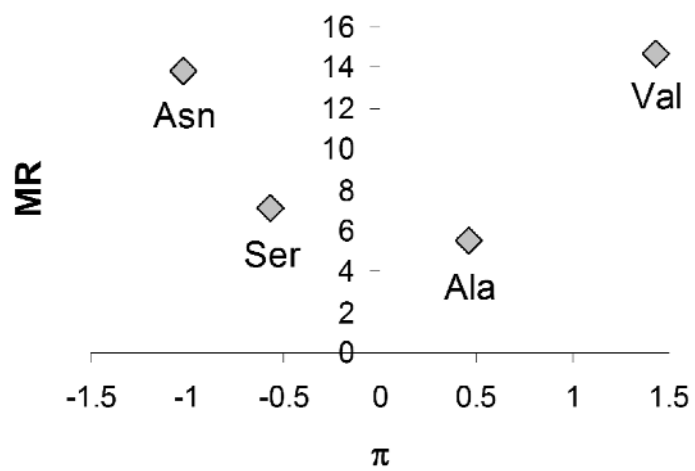


Figure 4.
 π and MR values for selected amino acids.

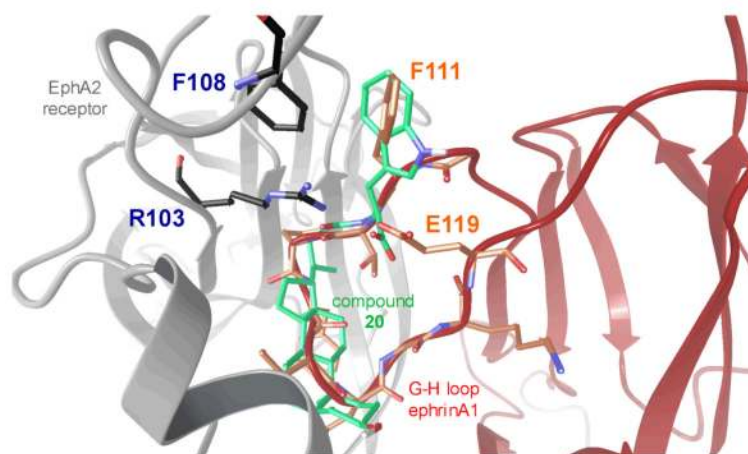


Figure 5. Compound 20 (green carbons) within the ligand binding channel of EphA2 (grey cartoon representation). The structure of ephrin-A1 ligand is also displayed (red cartoon representation), as it appears in the X-ray structure of the EphA2-ephrin-A1 complex.³⁴

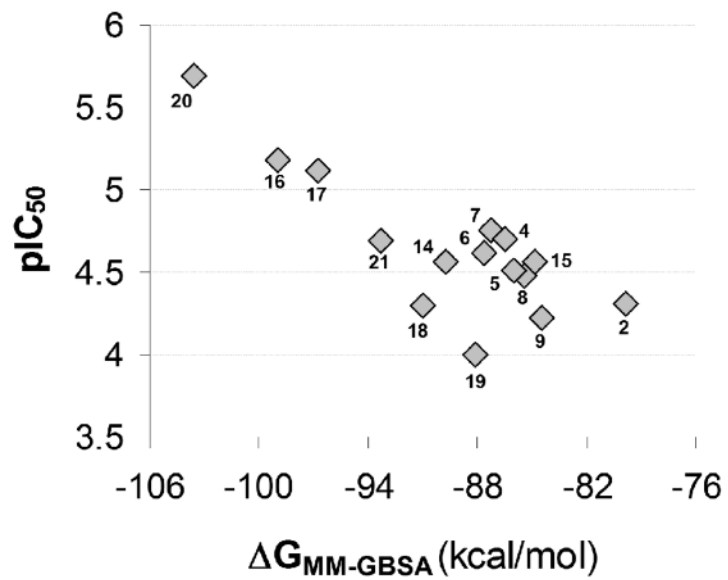


Figure 6. Plot of experimental pIC₅₀ values versus calculated ΔG of binding from MM-GBSA calculations.

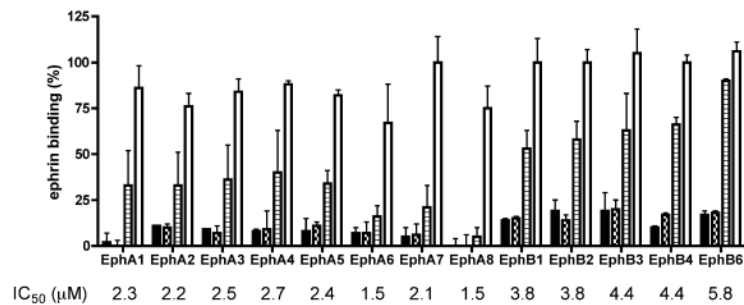


Figure 7.

Compound 20 dose-dependently displaces the binding of ephrin-A1-Fc and the ephrin-B1-Fc ectodomains from immobilized EphA-Fc or EphB-Fc ectodomains, respectively. Tested concentrations: 30 μM (black bar), 10 μM (checked bar), 3 μM (striped bar), 1 μM (white bar). IC₅₀ values are means from at least three independent experiments. The error bars represent standard errors.

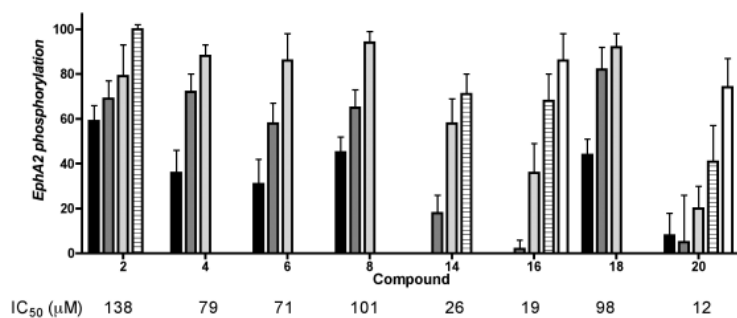


Figure 8.

Relative EphA2 phosphorylation in presence of different concentrations of selected compounds: 100 μ M (black bar), 50 μ M (dark gray bar), 25 μ M (light gray bar), 12 μ M (striped bar), 6 μ M (white bar). EphA2 phosphorylation was induced by treatment of PC3 cells with 0.25 μ g/mL-1 ephrin-A1-Fc. Cells were pretreated for 20 minutes with 1% DMSO or the indicated concentration of compounds and then stimulated for 20 minutes with ephrin-A1-Fc. Data are reported as a mean \pm SEM of at least three independent experiments. EphA2 phosphorylation in cells treated with ephrin-A1-Fc was arbitrarily assigned a value of 100, and in cells treated with Fc a value of 0.

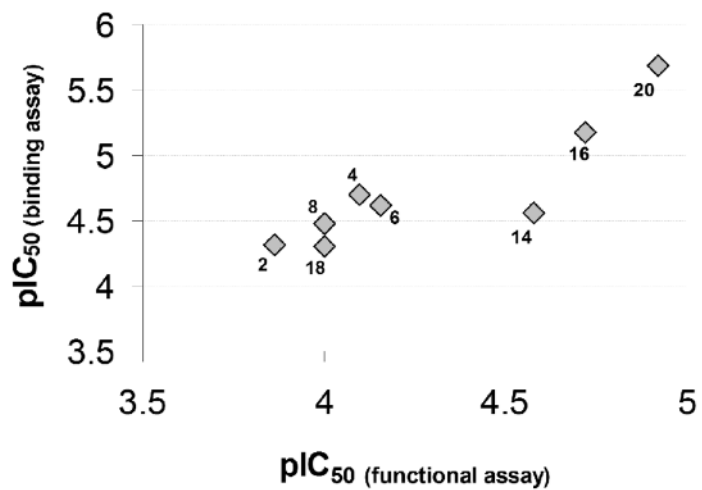


Figure 9. Plot of pIC₅₀ values obtained in the binding assay with purified EphA2 receptor versus those measured for EphA2 phosphorylation in PC3 cells.

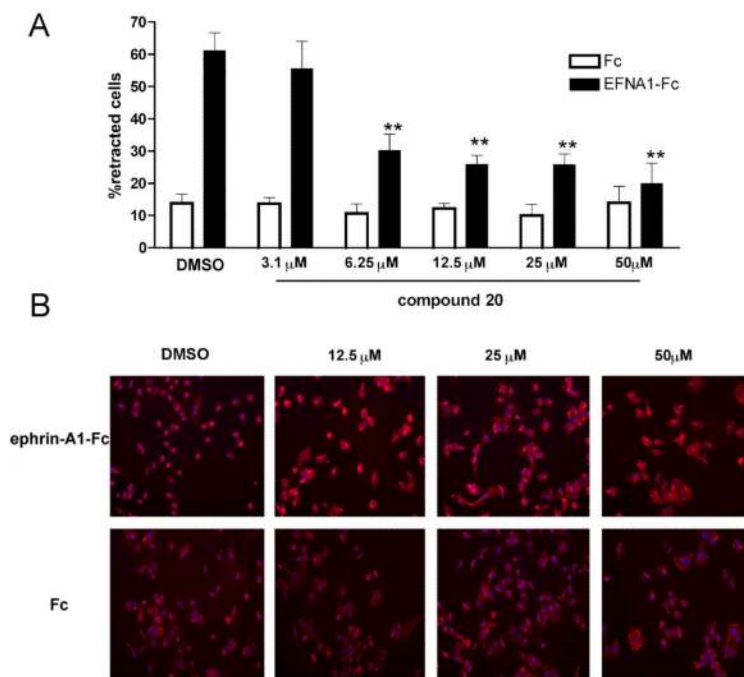
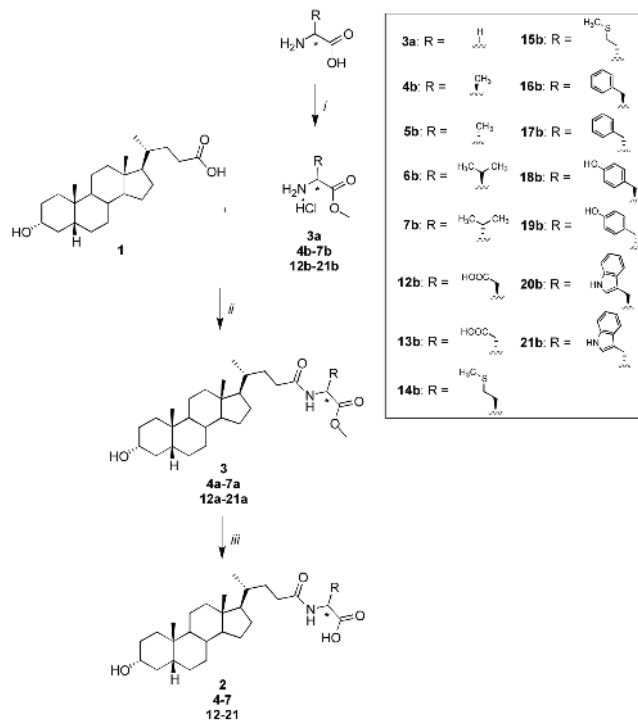


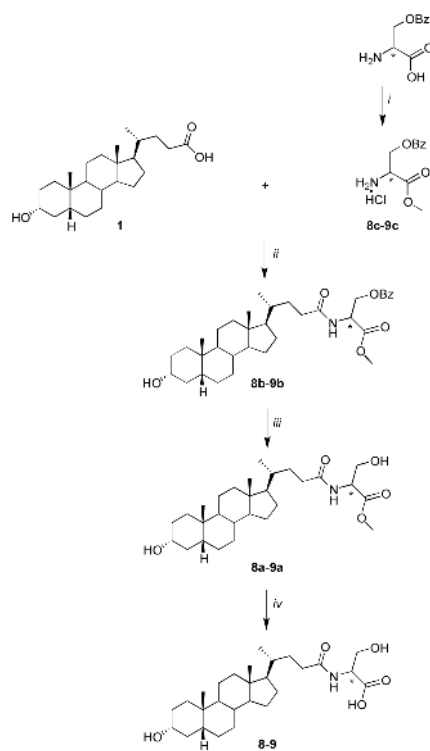
Figure 10.

Inhibition of cell-retraction and rounding in PC3 cells by compound 20. A) Dose-response curve for compound 20 in presence of ephrin-A1-Fc (black bar), or Fc alone (white bar) as a control. The histogram shows the average percentage of retracting cells \pm standard error. Cells having rounded shape and decreased spreading were scored as retracting. The percentages of cell retraction under different conditions were compared with those stimulated with ephrin-A1-Fc + DMSO by one-way ANOVA followed by Dunnett's post test. **: $p < 0.01$. B) Representative pictures of PC3 cells morphology variation. PC3 cells were pretreated for 15 min with the indicated concentrations of compound 20 (μ M) and then stimulated with 0.5 μ g/ml ephrin-A1-Fc or Fc alone as a control for 10 min in presence of the compound. Cells were stained with rhodamine-phalloidin to label actin filaments (red) and 4',6-diamidino-2-phenylindole (DAPI) to label nuclei (blue). DMSO was used as a control.

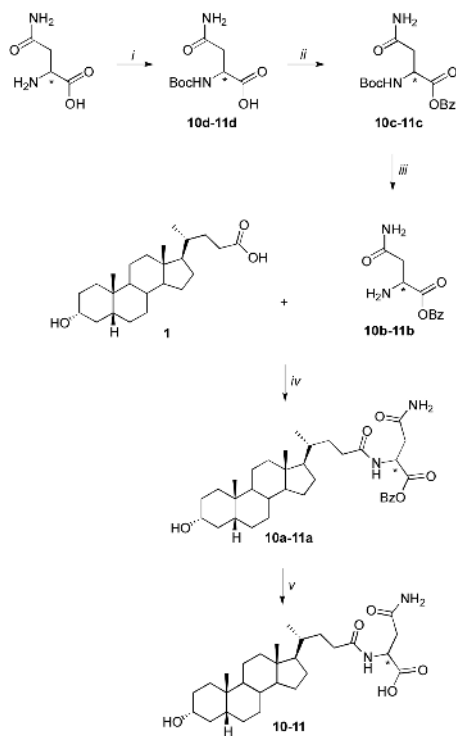


Scheme 1.

Reagents and conditions: i) Acetyl chloride, MeOH, from 0 °C to reflux, overnight; ii) NMM, EDCI, CH₂Cl₂, r.t., overnight ; iii) NaOH_(aq) 15%, EtOH, r.t. 1 h.

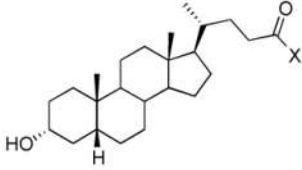
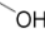
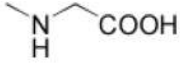
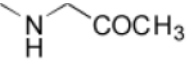
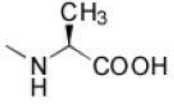
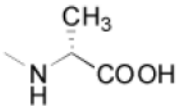
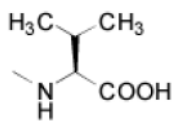
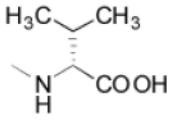
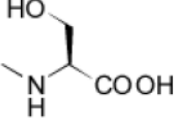
**Scheme 2.**

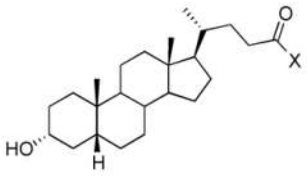
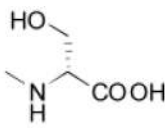
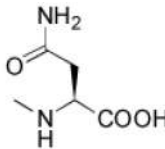
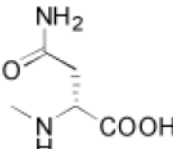
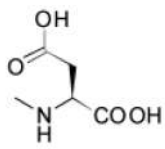
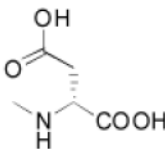
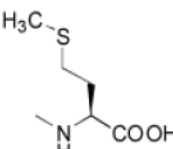
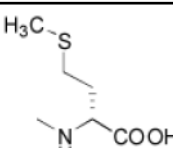
Reagents and conditions: i) Acetyl chloride, MeOH, from 0 °C to reflux, overnight; ii) NMM, EDCl, CH₂Cl₂ dry, r.t. overnight; iii) Pd/C 10%, MeOH, H₂, 30 psi, 3 h; iv) NaOH_(aq) 15%, EtOH, r.t., 1 h.

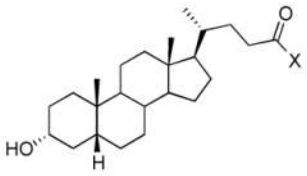
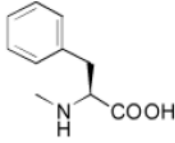
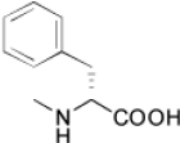
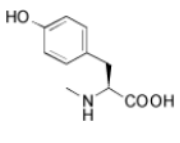
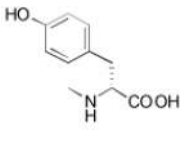
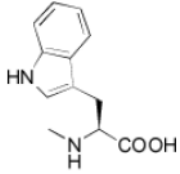
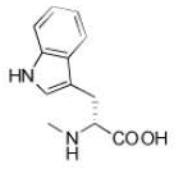
**Scheme 3.**

Reagents and conditions: i) Boc₂O, Na₂CO₃, 1,4-dioxane, water, r.t., overnight; ii) Cs₂CO₃, MeOH, BzBr, DMF, r.t., overnight; iii) TFA, CH₂Cl₂, r.t., overnight; iv) NMM, EDCI, CH₂Cl₂ dry, r.t., overnight; v) Pd/C 10%, MeOH, H₂, 30 psi, 3 h.

Table 1pIC₅₀ and physicochemical descriptors (π , MR) for amino acid conjugates of LCA

				
Cpd.	X	pIC ₅₀ ± SEM ^a	π ^b	MR ^b
1 (LCA)		4.24 ± 0.07	-	-
2		4.31 ± 0.09	0	1.03
3		< 3.50	0	1.03
4		4.70 ± 0.20	0.46	5.51
5		4.51 ± 0.09	0.46	5.51
6		4.62 ± 0.05	1.43	14.69
7		4.76 ± 0.11	1.43	14.69
8		4.48 ± 0.03	-0.57	7.14

				
Cpd.	X	pIC ₅₀ ± SEM ^a	π ^b	MR ^b
9		4.22 ± 0.09	-0.57	7.14
10		<3.50	-1.0	13.85
11		<3.50	-1.0	13.85
12		<3.50	-0.29	12.54
13		<3.50	-0.29	12.54
14		4.56 ± 0.10	1.12	22.21
15		4.56 ± 0.12	1.12	22.21

				
Cpd.	X	pIC ₅₀ ± SEM ^a	π ^b	MR ^b
16		5.18 ± 0.12	2.00	30.91
17		5.12 ± 0.07	2.00	30.91
18		4.30 ± 0.16	1.69	32.24
19		4.00 ± 0.11	1.69	32.24
20		5.69 ± 0.12	2.36	41.33
21		4.69 ± 0.03	2.36	41.33

^aValues are means ± standard error of the mean (SEM) from at least three independent experiments.

^bπ and MR descriptors for conjugating amino acids of **2-21** were calculated with MOE software.³³